JOURNAL OF SOLID STATE CHEMISTRY **111**, 315–321 (1994)

A Mixed-Valent Molybdenum Monophosphate with a "Butterfly"-Shaped Tunnel Structure $Cs_6Mo_7O_9(PO_4)_7 \cdot H_2O$

A. Guesdon, M. M. Borel, A. Leclaire, A. Grandin, and B. Raveau

Laboratoire CRISMAT, Associé au CNRS, ISMRA, Université de Caen, Boulevard du Maréchal Juin 1450 Caen Cedex, France

Received May 6, 1993; in revised form September 28, 1993; accepted September 30, 1993

A new mixed-valent molybdenum monophosphate $Cs_6Mo_7O_9(PO_4)_7 \cdot H_2O$ has been isolated by solid state chemistry. It crystallizes in the space group *Pnma* with $a = 10.084(1)$ Å, $b = 21.297(3)$ Å, $c = 17.491(1)$ Å. Its framework $[Mo_7P_7O_{37}]_\infty$ consists of two kinds of structural units formulated $Mo_4P_6O_{30}$ and Mo_3PO_{16}. The $Mo_4P_6O_{30}$ units are built up from two edge-sharing MoO_6 octahedra sharing their corners with two other MoO_6 octahedra and six PO_4 tetrahedra, whereas the Mo_3PO_{16} units, which also exhibit two edge-sharing octahedra, can be derived from the first type of units by removing one octahedron and five tetrahedra. The structure can then be described by the association of $[Mo_4P_6O_{28}]_\infty$ layers, built up of corner-sharing $Mo_4P_6O_{30}$ units, with $[Mo_3PO_{15}]_\infty$ chains, built up of corner-sharing Mo_3PO_{16} units. A comparison with leucophosphite is made. The host lattice $[Mo_7P_7O_{37}]_\infty$ delimits two kinds of tunnels running along a: a large butterfly-shaped tunnel where the Cs^+ ions and H_2O molecules are located, and smaller tunnels occupied by Cs^+ ions only. Besides these tunnels, cages are also obtained, fully occupied by Cs^+ ions. The ordered distribution of Mo(V) and Mo(IV) species is also demonstrated: Mo(V) sits in MoO_6 octahedra that exhibit one free apex, whereas Mo(IV) sits in the edge-sharing octahedra of the $Mo_4P_6O_{30}$ units.

INTRODUCTION

Investigations performed over the past ten years on Mo(V) phosphates have allowed the synthesis of a large number of pentavalent molybdenum compounds, compared to pure octahedral structures where Mo(V) oxides are very rare. This ability of mixed frameworks to stabilize Mo(V) is mainly explained by their ability to form MoO_6 octahedra involving a free apex, by introducing large cations such as potassium, rubidium, or cesium. The latter characteristic is necessary to stabilize the molybdenyl ion, which requires an abnormally short Mo–O bond. On the other hand, the mixed valence of molybdenum involving Mo(V) is very rare in these phosphates. Only two cesium phosphates, $CsMo_2P_2O_{10}$ (1) and $Cs_{1.5}Mo_2P_2O_{11}$ (2), which correspond to the mixed valences Mo(IV)/Mo(V) and Mo(V)/Mo(VI), respectively, have been isolated up to now.

In order to understand this unusual behavior of the cesium phosphates, a detailed investigation of the system Cs–P–Mo–O has been undertaken. We report here on the synthesis and structural study of a novel moxed-valent molybdenum phosphate, $Cs_6Mo_7O_9(PO_4)_7 \cdot H_2O$.

SYNTHESIS

Single crystals of this phase were grown from a mixture of nominal composition $Cs_2Mo_2P_2O_{11}$.

The synthesis was performed in two steps starting from a mixture in adequate ratios to obtain $Cs_2Mo_2P_2O_{11}$. First an adequate mixture of Cs_2CO_3, $H(NH_4)_2PO_4$, and MoO_3 according to the composition $Cs_2P_2Mo_{1.67}O_{11}$ was ground and heated to 673 K in air to eliminate CO_2, H_2O, and NH_3. In the second step the appropriate amount of metallic molybdenum was added and the finely ground mixture was placed in an alumina tube sealed in an evacuated silica ampoule and was then heated for 1 day to 1123 K and cooled at 2 K per hour to 923 K. The sample was finally quenched to room temperature. In the resulting mixture, some dark brown crystals were extracted. The microprobe analysis of these crystals confirmed the composition $Cs_6Mo_7P_7$ in agreement with the structure determination.

Subsequently the synthesis of the pure phase $Cs_6Mo_7P_7O_{37} \cdot H_2O$ was performed in a similar way in two steps but starting from the exact stoichiometric composition. The second step was carried out in that case during 1 day at 823 K, the water coming from the atmosphere.

The powder X-ray diffraction pattern was indexed in an orthorhombic cell (Table 1) in agreement with the parameters obtained from the single crystal study.

The presence of water has been shown by the infrared spectra registered with a Nicolet 60 SX spectrometer and confirmed by thermogravimetric analysis. The latter showed the reversible character of the hydratation: the material loses H_2O at 500 K and reabsorbs atmospheric water at room temperature.

0022-4596/94 $6.00

TABLE 1

Interreticular Distances for $Cs_6Mo_7P_7O_{37} \cdot H_2O$

h k l	d_{calc} (Å)	d_{obs} (Å)	I_o	*h k l*	d_{calc} (Å)	d_{obs} (Å)	I_o
0 0 2	8.745	8.707	32.6	1 7 3	2.606	2.604	33.6
1 0 1	8.736			1 3 6	2.605		
0 2 2	6.758	6.724	73.9	2 7 0	2.605		
1 2 1	6.754			2 6 3	2.598	2.592	12.2
0 4 0	5.324	5.324	22.3	3 2 4	2.585	2.582	20.1
1 3 2	4.836	4.835	26.1	0 8 2	2.547	2.546	20.8
0 4 2	4.548	4.547	35.3	1 8 1	2.547		
1 4 1	4.546			3 5 2	2.526	2.525	35.2
2 2 1	4.410	4.390	18.8	2 0 6	2.524		
0 0 4	4.373			0 1 7	2.482	2.486	22.5
2 0 2	4.368	4.354	26.3	0 3 7	2.357	2.355	15.0
2 1 2	4.279	4.260	18.4	1 8 3	2.355		
0 5 1	4.139	4.130	78.5	2 8 0	2.354		
2 3 1	4.002	4.002	25.7	4 3 1	2.354		
1 5 1	3.829	3.823	20.8	2 0 7	2.239	2.237	25.4
2 4 0	3.661	3.652	21.1	1 7 5	2.238		
1 5 2	3.580	3.578	69.6	2 7 4	2.238		
0 5 3	3.439	3.440	23.2	3 7 1	2.237		
3 0 1	3.301	3.300	44.5	2 1 7	2.227	2.225	17.0
1 5 3	3.255	3.253	44.7	4 2 5	2.008	2.007	13.6
2 5 0	3.254			2 0 8	2.006		
1 4 4	3.204	3.200	88.9	3 0 7	2.005		
2 5 1	3.199			3 7 4	2.005		
1 2 5	3.156	3.154	100	0 8 6	1.966	1.965	13.5
2 2 4	3.155			4 3 5	1.965		
3 2 1	3.153			5 0 2	1.965		
0 3 5	3.138	3.133	49.1	3 8 3	1.965		
3 0 2	3.138			0 7 7	1.931	1.930	16.4
1 6 2	3.127			2 3 8	1.930		
3 3 1	2.993	2.991	39.5	3 3 7	1.930		
1 6 3	2.904	2.907	51.4	1 8 6	1.929		
2 2 5	2.775	2.774	16.2	4 7 1	1.929		
3 1 4	2.644	2.640	11.9				

STRUCTURE DETERMINATION

A dark brown crystal with dimensions 0.045 × 0.039 × 0.032 mm^3 was selected for the structure determination. The cell parameters were determined and refined by diffractometric technique at 294 K with a least-squares refinement based upon 25 reflections with $18° < \theta < 22°$. The data were collected on a CAD4 Enraf–Nonius diffractometer with the data collection parameters of Table 2.

The reflections were corrected for Lorentz, polarization, and absorption effects. The structure was solved by the heavy atom method.

The small number of $I > 3\sigma(I)$ does not allow us to refine the anisotropic thermal factor of all the atoms.

The refinement of the coordinates and anisotropic thermal factors for Cs(1), Cs(2), Cs(3), and Cs(4) and isotropic thermal factors for the other atoms led to $R = 0.044$ and $R_w = 0.047$.

The positional parameters and B are tabulated in Table 3. Selected bond distances (Å) and angles (°) are given in Table 4.

DESCRIPTION OF THE STRUCTURE AND DISCUSSION

The projection of the structure of this mixed-valent phosphate onto the (100) plane (Fig. 1) shows that the $[Mo_7P_7O_{37}]_\infty$ host lattice consists of single PO_4 tetrahedra sharing their apices with MoO_6 octahedra. The MoO_6 octahedra share sometimes one apex, sometimes one edge. This framework delimits two kinds of tunnels running along **a**: very large tunnels with an unusual shape, looking like a butterfly, and smaller tunnels forming pairs.

In fact the $[Mo_7P_7O_{37}]_\infty$ host lattice can be described from two sorts of structural units:

(i) $Mo_4P_6O_{30}$ units (Fig. 2a) that are built up from two edge-sharing MoO_6 octahedra, sharing their two common apices with two other MoO_6 octahedra so that two oxygen

TABLE 2

Summary of Crystal Data, Intensity Measurements, and Structure Refinement Parameters for $Cs_6Mo_7P_7O_{37} \cdot H_2O$

Crystal data	
Space group	*Pnma*
Cell dimensions (Å)	a = 10.084(1) b = 21.297(3) c = 17.491(1)
Volume	3756.2(8) $Å^3$
Z	4
d_{calc}	4.05
d_{exp}	3.95
Intensity measurements	
λ (Mo$K\alpha$) (Å)	0.71073
Scan mode	$\omega - 5/3\ \theta$
Scan width (°)	$1 + 0.35 \tan\theta$
Slit aperture (mm)	$1.10 + \tan\theta$
max θ (°)	45
Standard reflections	3 (every 3000 sec)
Reflections with $I > 3\sigma$	819
μ (mm^{-1})	8.3
Structure solution and refinement	
Parameters refined	143
Agreement factors	$R = 0.044$, $R_w = 0.047$
Weighting scheme	$w = f(\sin\theta/\lambda)$
Δ/σ max	< 0.02
$\Delta\rho$ ($eÅ^{-3}$)	< 2.9

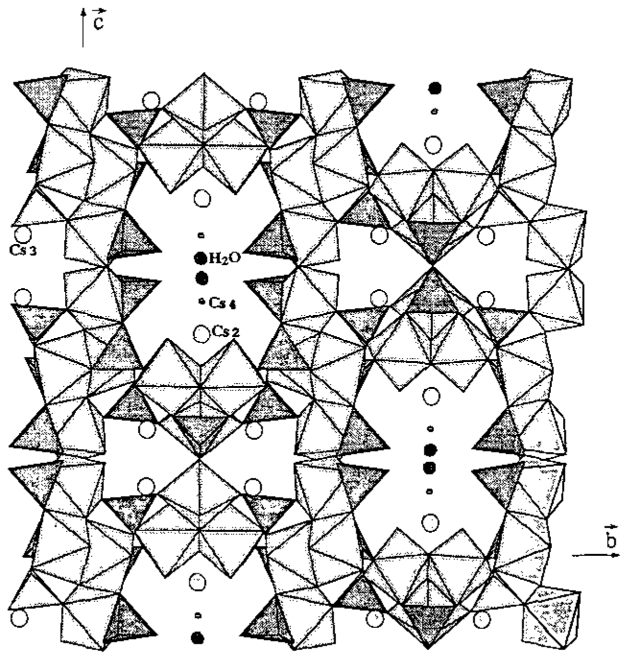

FIG. 1. Projection of the structure along **a** showing the stacking of the $[Mo_4P_6P_{28}]_\infty$ layers joined by the $[Mo_3PO_{15}]_\infty$ chains and showing the "butterfly"-shaped tunnels.

TABLE 3

Positional Parameters and Their Estimated Standard Deviations

Atom	x	y	z	$B(Å^2)$
Cs(1)	0.4553(3)	0.0380(1)	0.6085(1)	1.29(4)
Cs(2)	0.1872(5)	0.25	0.5811(3)	3.1(1)
Cs(3)	0.3713(3)	0.1342(1)	0.1737(2)	2.92(6)
Cs(4)	0.2440(6)	0.25	0.8323(3)	4.2(1)
Mo(1)	0.0376(3)	0.1889(1)	0.0216(2)	0.42(4)*
Mo(2)	0.0763(3)	0.0425(1)	0.5152(2)	0.33(4)*
Mo(3)	0.1494(3)	0.9875(1)	0.3150(2)	0.40(4)*
Mo(4)	0.2625(5)	0.25	0.3519(3)	0.66(8)*
P(1)	0.130(1)	0.0931(4)	0.6974(5)	0.3(2)*
P(2)	0.286(1)	0.0833(4)	0.9759(6)	0.9(2)*
P(3)	0.2993(9)	0.1030(4)	0.4006(5)	0.3(2)*
P(4)	0.080(1)	0.25	0.1870(8)	0.4(2)*
O(1)	0.479(2)	0.179(1)	0.568(1)	1.0(4)*
O(2)	0.171(4)	0.25	0.004(2)	1.3(7)*
O(3)	−0.064(2)	0.109(1)	0.058(1)	0.5(4)*
O(4)	0.193(2)	0.127(1)	0.014(1)	1.1(5)*
O(5)	−0.105(3)	0.25	0.062(2)	0.4(6)*
O(6)	0.098(2)	0.191(1)	0.139(1)	0.8(4)*
O(7)	−0.066(2)	0.105(1)	0.509(1)	1.0(5)*
O(8)	0.154(3)	0.083(1)	0.611(1)	1.2(5)*
O(9)	0.037(2)	0.006(1)	0.411(1)	0.4(4)*
O(10)	0.182(2)	0.108(1)	0.454(1)	0.3(4)*
O(11)	0.229(2)	−0.016(1)	0.515(1)	0.9(4)*
O(12)	0.123(4)	0.25	0.403(2)	0.9(6)*
O(13)	0.176(4)	0.25	0.251(2)	1.6(7)*
O(14)	0.279(2)	0.158(1)	0.344(1)	0.8(5)*
O(15)	0.437(4)	0.25	0.280(2)	1.1(7)*
O(16)	0.091(3)	1.046(1)	0.262(1)	1.8(5)*
O(17)	0.018(2)	0.924(1)	0.282(1)	1.0(5)*
O(18)	0.273(2)	0.955(1)	0.240(1)	1.1(5)*
O(19)	0.301(2)	1.040(1)	0.360(1)	0.5(4)*
O(20)	0.236(2)	0.920(1)	0.392(1)	0.4(4)*
O(21)	0.162(3)	0.159(1)	0.720(1)	1.2(5)*
OH2	0.438(6)	0.25	0.727(3)	4(1)*

Note. Starred atoms were refined isotropically. Anisotropically refined atoms are given in the form of the isotropic equivalent displacement parameter defined as $B = \frac{4}{3} \sum_i \sum_j \mathbf{a}_i \cdot \mathbf{a}_j \cdot \beta_{ij}$.

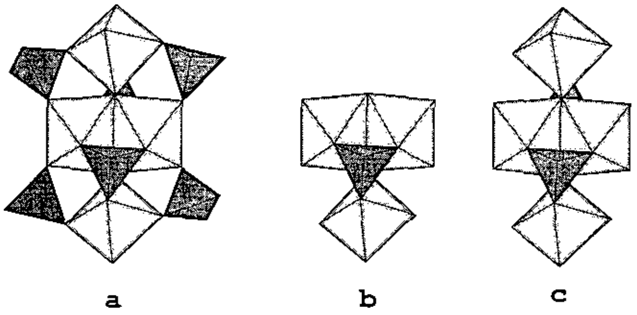

FIG. 2. Polyhedral units. (a) $Mo_4P_6O_{30}$ unit forming the $[Mo_4P_6O_{28}]_\infty$ layers; (b) Mo_3PO_{16} unit; (c) $Mo_4P_2O_{14}$ unit of the leucophosphite type structure.

TABLE 4

Distances (Å) and Angles (°) in the Octahedra and Tetrahedra for $Cs_6Mo_7P_7O_{37} \cdot H_2O$

Mo(1)	O(1^{i})	O(2)	O(3)	O(4)	O(5)	O(6)
O(1^{i})	1.69(3)	2.76(4)	2.70(4)	2.83(4)	2.85(4)	3.82(5)
O(2)	100(2)	1.90(3)	3.95(5)	2.64(3)	2.97(5)	2.79(5)
O(3)	91(1)	163(1)	2.09(2)	2.74(4)	3.04(2)	2.78(4)
O(4)	98(1)	84(1)	83(1)	2.06(3)	4.08(5)	2.75(4)
O(5)	99(1)	97(1)	94.0(9)	164(1)	2.06(3)	2.75(4)
O(6)	173(1)	87(1)	82(1)	82(1)	82(1)	2.14(2)
Mo(2)	O(7)	O(8)	O(9^{ii})	O(9)	O(10)	O(11)
O(7)	1.95(3)	2.89(4)	2.77(4)	2.90(3)	2.68(4)	3.93(4)
O(8)	93(1)	2.04(3)	2.74(4)	4.04(4)	2.81(4)	2.80(4)
O(9^{ii})	88(1)	85(1)	2.02(2)	3.23(5)	4.06(4)	2.99(3)
O(9)	94(1)	168(1)	105.9(8)	2.02(2)	2.73(3)	2.70(4)
O(10)	84(1)	86(1)	167.8(9)	84(1)	2.06(2)	2.90(4)
O(11)	175(1)	88(1)	97(1)	85(1)	91(1)	1.98(3)
Mo(3)	O(9^{iii})	O(16)	O(17)	O(18)	O(19)	O(20)
O(9^{iii})	2.06(2)	2.79(4)	2.85(3)	3.97(4)	2.89(4)	2.74(4)
O(16)	96(1)	1.66(3)	2.73(4)	2.70(4)	2.72(4)	3.81(4)
O(17)	90(1)	96(1)	1.98(3)	2.76(4)	4.00(4)	2.93(4)
O(18)	167(1)	97(1)	90(1)	1.94(3)	2.78(4)	2.79(4)
O(19)	89.6(9)	94(1)	170(1)	88(1)	2.04(3)	2.68(4)
O(20)	81(1)	173(1)	90(1)	86(1)	79(1)	2.15(2)
Mo(4)	O(5^{iv})	O(12)	O(13)	O(14)	O(14^{v})	O(15)
O(5^{iv})	2.02(4)	2.81(5)	3.96(6)	2.82(4)	2.82(4)	2.80(5)
O(12)	99(2)	1.66(4)	2.71(6)	2.72(4)	2.72(4)	3.83(6)
O(13)	165(2)	96(2)	1.98(5)	2.77(4)	2.77(4)	2.68(6)
O(14)	89.7(8)	96.1(8)	88.7(8)	1.98(3)	3.94(6)	2.78(4)
O(14^{v})	89.7(8)	96.1(8)	88.7(8)	168(2)	1.98(3)	2.78(4)
O(15)	84(2)	177(2)	81(2)	83.9(8)	83.9(8)	2.16(4)

P(1)	O(8)	O(17^{vi})	O(18^{vii})	O(21)
O(8)	1.55(3)	2.56(4)	2.51(4)	2.51(4)
O(17^{vi})	110(2)	1.58(3)	2.58(4)	2.54(4)
O(18^{vii})	105(2)	109(2)	1.60(3)	2.54(4)
O(21)	111(2)	111(2)	110(2)	1.50(3)
P(2)	O(4^{viii})	O(7^{ix})	O(11^{x})	O(20^{vii})
O(4^{viii})	1.48(3)	2.50(4)	2.49(4)	2.47(4)
O(7^{ix})	110(2)	1.58(3)	2.53(4)	2.50(4)
O(11^{x})	108(2)	106(2)	1.59(3)	2.54(4)
O(20^{vii})	112(2)	109(2)	111(2)	1.49(3)
P(3)	O(3^{xi})	O(10)	O(14)	O(19^{xii})
O(3^{xi})	1.56(3)	2.57(4)	2.56(4)	2.45(3)
O(10)	113(1)	1.51(3)	2.40(4)	2.51(4)
O(14)	111(1)	103(1)	1.54(3)	2.53(4)
O(19^{xii})	106(1)	111(1)	112(1)	1.53(3)
P(4)	O(6)	O(6^{v})	O(13)	O(15^{i})
O(6)	1.52(3)	2.52(6)	2.45(5)	2.50(5)
O(6^{v})	112(2)	1.52(3)	2.45(5)	2.50(5)
O(13)	110(1)	110(1)	1.47(5)	2.47(6)
O(15^{i})	108(1)	108(1)	109(2)	1.56(5)

Cs(1)–O(1)	3.10(3)	Cs(1)–O(20^{xiii})	3.23(3)
Cs(1)–O(3^{x})	3.43(2)		
Cs(1)–O(3^{xi})	3.28(2)	Cs(2)–O(1)	3.31(3)
Cs(1)–O(8)	3.18(3)	Cs(2)–O(1^{v})	3.31(3)
Cs(1)–O(11)	3.04(3)	Cs(2)–O(5^{iv})	3.26(4)
Cs(1)–O(16^{vii})	3.27(3)	Cs(2)–O(12)	3.18(4)
Cs(1)–O(17^{vii})	3.15(3)	Cs(2)–O(21)	3.12(3)
Cs(1)–O(18^{vii})	3.25(3)	Cs(2)–O(21^{v})	3.12(3)
Cs(1)–O(19^{xiii})	3.01(3)		

TABLE 4—*Continued*

Cs(3)–O(4)	3.32(3)	Cs(4)–O(2^{viii})	3.08(4)
Cs(3)–O(6)	3.07(3)	Cs(4)–O(21)	2.87(3)
Cs(3)–O(7^{xi})	3.31(3)	Cs(4)–O(21^{v})	2.87(3)
Cs(3)–O(13)	3.43(3)	Cs(4)–OH_2	2.68(6)
Cs(3)–O(14)	3.17(3)	Cs(4)–OH_2^{xv}	3.26(7)
Cs(3)–O(15)	3.16(2)		
Cs(3)–O(16^{xiv})	3.11(3)		

Symmetry code

i	$-1/2 + x$	y	$1/2 - z$	ix	$1/2 + x$	y	$3/2 - z$
ii	$-x$	$-y$	$1 - z$	x	$1/2 - x$	$-y$	$1/2 + z$
iii	x	$1 + y$	z	xi	$1/2 + x$	y	$1/2 - z$
iv	$1/2 + x$	$1/2 - y$	$1/2 - z$	xii	x	$-1 + y$	z
v	x	$1/2 - y$	z	xiii	$1 - x$	$1 - y$	$1 - z$
vi	$-x$	$1 - y$	$1 - z$	xiv	$1/2 + x$	$-1 + y$	$1/2 - z$
vii	$1/2 - x$	$1 - y$	$1/2 + z$	xv	$-1/2 + x$	$1/2 - y$	$3/2 - z$
viii	x	y	$1 + z$				

atoms are triply bonded. In these units four PO_4 tetrahedra share two of their corners with the MoO_6 octahedra, whereas each of the two remaining PO_4 tetrahedra shares three corners with the MoO_6 octahedra.

(ii) Mo_3PO_{16} units (Fig. 2b) that are built up from two edge-sharing MoO_6 octahedra, sharing one of their common apices with one MoO_6 octahedron so that one oxygen atom is triply bonded. In these units the PO_4 tetrahedron shares three of its apices with the apical oxygens of the three MoO_6 octahedra. Note that this unit is deduced from the $Mo_4P_6O_{30}$ unit by removing five PO_4 tetrahedra and one MoO_6 octahedron.

In the (010) plane each $Mo_4P_6O_{30}$ unit is linked to four other identical units in such a way that two MoO_6 octahedra and two PO_4 tetrahedra of one unit are connected to two PO_4 tetrahedra and two MoO_6 octahedra of the four surrounding identical units, forming $[Mo_4P_6O_{28}]_\infty$ layers (Fig. 3). The view of the structure along **a** (Fig. 1) shows that these layers are connected through Mo_3PO_{16} units; more exactly the Mo_3PO_{16} units share the corners of their

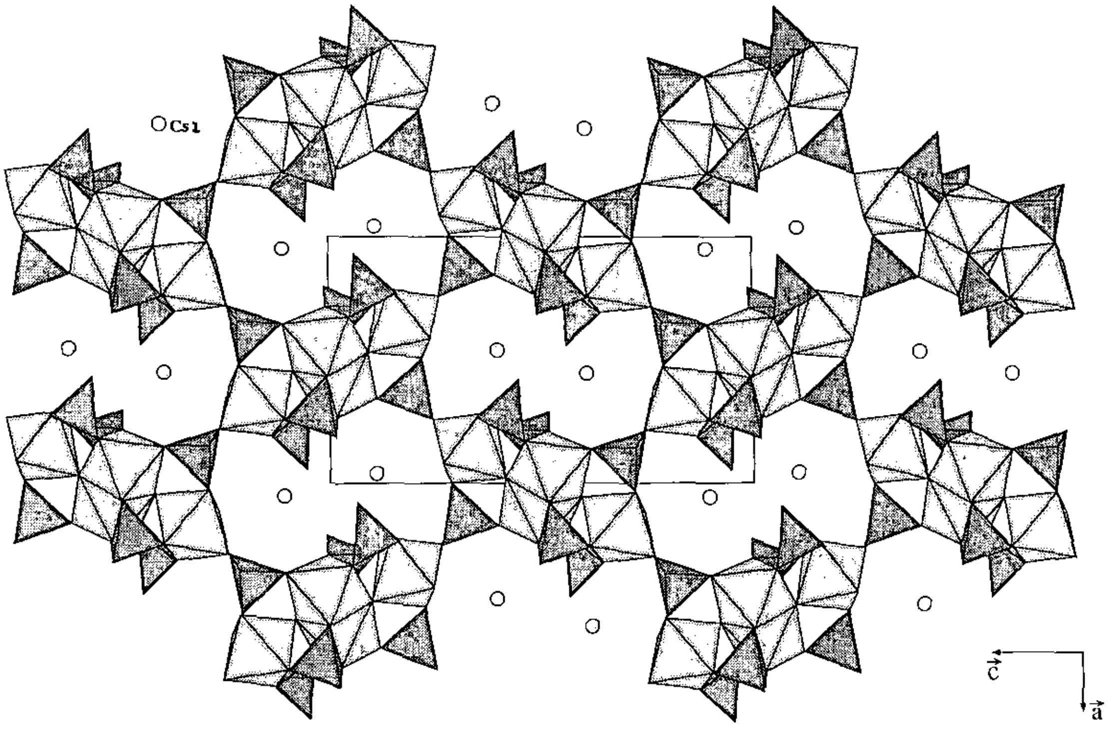

FIG. 3. $[Mo_4P_6O_{28}]_\infty$ layer viewed along **b**.

polyhedra forming infinite zigzag $[Mo_3PO_{15}]_\infty$ chains running along **a** (Fig. 4). As a result the host lattice $[Mo_7P_7O_{37}]_\infty$ can be described as the assemblage of $[Mo_4P_6O_{28}]_\infty$ layers parallel to (010) with $[Mo_3PO_{15}]_\infty$ chains running along **a** in such a way that one $Mo_4P_6O_{30}$ unit is linked to four Mo_3PO_{16} units.

The $[Mo_4P_6O_{28}]_\infty$ layers exhibit some similarity with the leucophosphite structure $AMo_2P_2O_{10} \cdot H_2O$ ($A = NH_4$, Rb) (3, 4) for which similar $Mo_4P_6O_{30}$ units built up from Mo_4O_{20} units bridged with PO_4 tetrahedra have been observed (Fig. 5). Nevertheless, it can be seen that in the leucophosphite structure, the $Mo_4P_6O_{30}$ units are interpenetrated (Fig. 5), whereas they share the apices of their polyhedra in the phosphate $Cs_6Mo_7O_9(PO_4)_7 \cdot H_2O$ (Fig. 3). Consequently, the leucophosphite structure is described in terms of $Mo_4P_2O_{14}$ units (Fig. 2c) which are derived from the $Mo_4P_6O_{30}$ units by elimination of four PO_4 tetrahedra. Thus both the $[Mo_4P_6O_{28}]_\infty$ layers and the leucophosphite structure could be described as the assemblages of identical $Mo_4P_2O_{14}$ units with PO_4 tetrahedra, but the relative arrangement of these units and of the PO_4 tetrahedra is basically different in the two structures.

The PO_4 tetrahedra of the $Mo_4P_6O_{30}$ units, P(1), have one free corner directed toward the center of the butterfly tunnel; their other three corners are shared with three MoO_6 octahedra, i.e., two Mo(2) and Mo(3) octahedra of their own unit and one Mo(3) octahedron of the next $Mo_4P_6O_{30}$ unit. The P(2) and P(3) tetrahedra of the $Mo_4P_6O_{30}$ share their four apices with MoO_6 octahedra, i.e., with two Mo(2) and Mo(3) octahedra of their own $Mo_4P_6O_{30}$ unit, and with two Mo(1) and Mo(4) octahedra of the same Mo_3PO_{16} unit. The PO_4 tetrahedra, P(4), of the Mo_3PO_{16} units also share their four apices with MoO_6 octahedra, i.e., with three Mo(1) and Mo(4) octahedra of their own unit and one Mo(4) octahedron of the next Mo_3PO_{16} unit in the $[Mo_3PO_{15}]_\infty$ chain. The interatomic distances (Table 4) show that these tetrahedra are significantly distorted, with P–O distances ranging from 1.47 to 1.60 Å. This is in agreement with the large strains that exist in this structure owing to the association of the structural units $Mo_4P_6O_{30}$ and Mo_3PO_{16} which involve triply bonded oxygens. Nevertheless one must notice that the P(3) tetrahedra, which ensure the junction between the $Mo_4P_6O_{30}$ units and the Mo_3PO_{16} units, are less distorted, with P–O bonds ranging from 1.51 to 1.56 Å.

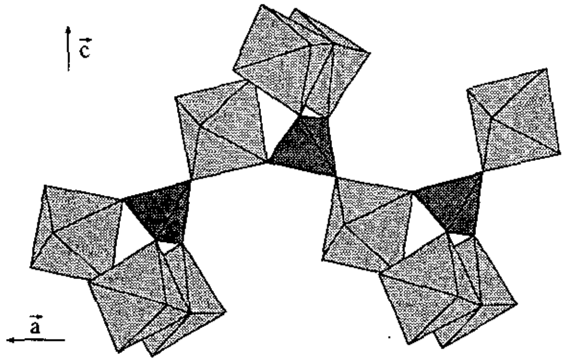

FIG. 4. $[Mo_3PO_{15}]_\infty$ zigzag chain.

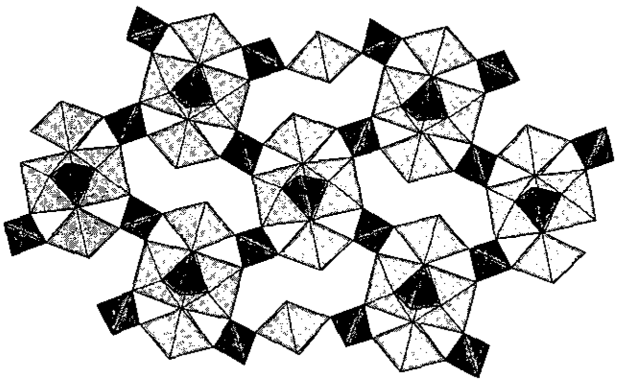

FIG. 5. $[MoP_2O_{10}]_\infty$ layer of the leucophosphite type structure.

The edge-sharing Mo(2) octahedra of the $Mo_4P_6O_{30}$ units do not exhibit any free apex (Fig. 2a) and are characterized by rather homogeneous Mo–O distances ranging from 1.95 to 2.26 Å (Table 4), suggesting that they correspond to Mo(IV). The valence calculations according to the Zachariasen model (5) confirm this hypothesis, with a value of 4.10 for the Mo(2) valence. Note also the very short Mo(2)–Mo(2) distance in the bioctahedra of 2.434 Å, close to that observed in the bioctahedral units of leucophosphite (6). The Mo(3) octahedra of the $Mo_4P_6O_{30}$ units have one free corner directed toward the center of the smaller tunnels (Fig. 1), whereas the four other apices are linked to two four tetrahedra and the last one is shared with two Mo(2) octahedra, i.e., is triply bonded. The valence calculations show that this molybdenum atom is pentava-

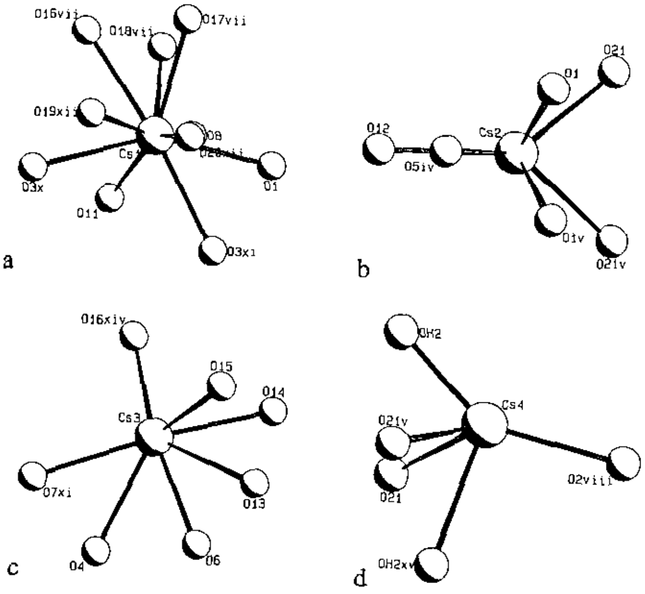

FIG. 6. The different Cs^+ environments.

lent (5.14). Indeed, the geometry of these octahedra is characteristic of Mo(V), with a very short Mo(3)–O bond of 1.66 Å, characteristic of the molybdenyl ion, and the longer Mo(3)–O distance of 2.15 Å corresponding to the opposed bond. The four other Mo(3)–O bonds are rather homogeneous (1.94 to 2.06 Å).

The Mo(1) and Mo(4) octahedra which form the Mo_3PO_6 units exhibit a geometry characteristic of Mo(V); they all have one free apex directed toward the center of the butterfly tunnels, characterized by a very short Mo–O bond of 1.69 Å for Mo(1) and 1.66 Å for Mo(4). The opposite distances are abnormally long (2.14 to 2.16 Å), whereas the intermediate Mo–O distances are rather homogeneous (Table 4). The pentavalent character of Mo(1) and Mo(4) is also confirmed by valence calculations which lead to values of 4.99 and 5.17 for Mo(1) and Mo(4), respectively. Note that the Mo(1)–Mo(1) distances of the edge-sharing octahedra which form the Mo_3PO_6 units are significantly larger (2.603 Å) than the Mo(2)–Mo(2) distances (2.43 Å) corresponding to edge-sharing octahedra in the $Mo_4P_6O_{30}$ units. This is in agreement with the higher coulombic repulsion introduced by Mo(V) on the Mo(1) sites, compared to that due to Mo(IV) on the Mo(2) sites.

As shown from the projection of the structure along **a** (Fig. 1) the butterfly-shaped tunnels are occupied by Cs(2) and Cs(4), and H_2O simultaneously and the smaller tunnels are occupied by Cs(3) only. The Cs(2) ions are surrounded by six oxygen atoms forming a trigonal pyramid (Fig. 6a) with Cs(2)–O distances ranging from 3.12 to 3.31 Å. Cs(4) exhibits a fivefold coordination (Fig. 6b) with three short Cs(4)–O distances (2.68–2.87 Å) and two longer ones (3.08–3.26 Å). It is in fact linked to two H_2O molecules and three oxygen atoms of the $[Mo_7P_7O_{37}]_\infty$ framework. Note the abnormally short Cs(2)–O distance of 2.68 Å between one H_2O molecule and Cs^+. Such small distances ranging from 2.68 to 2.95 Å have previously been observed in $Cs_{11}O_3$ (7). The Cs(3) ions sitting in the smaller tunnels are surrounded by seven oxygen atoms forming a ring around them (Fig. 6c), with Cs–O distances ranging from 3.07 to 3.43 Å (Table 4). Besides the tunnels there exist voluminous cages which result from the association of $Mo_4P_6O_{30}$ units in the $[Mo_4P_6O_{28}]_\infty$ layers (Fig. 3). The Cs(1) ions sit in those cages, where they are surrounded by ten oxygen atoms (Fig. 6a), with Cs–O distances ranging from 3.01 to 3.43 Å. The distances between the water molecule and the oxygen atoms are greater than 3.1 Å.

CONCLUDING REMARKS

This structural study shows the remarkable ability of cesium phosphates to stabilize the mixed-valent Mo(V)–Mo(IV), which corresponds to an ordered distribution of the Mo(V) and Mo(IV) species. The striking features of such a framework are the existence of large butterfly-shaped tunnels that are at the origin of its zeolitic properties, and the presence of strongly strained structural units. It appears clearly that association of the latter requires that some of PO_4 and MoO_6 polyhedra exhibit a free corner. Such a property might be due to the large size of cesium. This opens the route to the investigation of other microporous structures with a mixed valence of molybdenum by introducing larger cations using hydrothermal techniques.

REFERENCES

1. A. Guesdon, M. M. Borel, A. Leclaire, A. Grandin, and B. Raveau, *Z. Anorg. Allg. Chem.* **619,** 1841 (1993).
2. M. M. Borel, A. Leclaire, A. Grandin, and B. Raveau, *J. Solid State Chem.* **108,** 336 (1994).
3. H. E. King, Jr., L. A. Mundi, K. G. Strohmaier, and R. C. Haushalter, *J. Solid State Chem.* **92,** 1 (1991).
4. A. Leclaire, M. M. Borel, A. Grandin, and B. Raveau, *J. Solid State Chem.* **108,** 177 (1994).
5. W. H. Zachariasen, *J. Less-Common Met.* **62,** 1 (1978).
6. P. B. Moore, *Am. Mineral.* **57,** 397 (1972).
7. A. Simon and E. Westerbeck, *Z. Anorg. Allg. Chem.* **428,** 187 (1977).